




A Practical Nonlinear Strength Criterion for Rock Masses and Other Geological Materials

S. D. Cylwik¹ (✉) , J. R. Killian¹, and P. F. Cicchini²

¹ Call & Nicholas, Inc., Tucson, AZ, USA
scylwik@cni.tucson.com

² North Star Geotech, LLC, Tucson, AZ, USA

Abstract. Rock mass strength is a required input parameter for many types of analysis in both mining and civil engineering. This paper introduces a nonlinear formulation of the CNI method, an empirical rock mass strength criterion based on quantitative input parameters. Most of the input parameters to the CNI method are physical properties that can be directly measured in the laboratory or core shed. The nonlinear criterion is formulated in terms of compressive strength, friction angle, and a curvature coefficient. To determine typical values for the curvature coefficient, the generalized form of the nonlinear criterion is fit to published testing of intact hard rock, weak rock, saprolite, rock joints, rockfill, and sand. The nonlinear criterion is shown to effectively model all material types considered and provides a basis for empirical estimation of the curvature coefficient for rock mass. The strength criterion is evaluated for a range of rock mass conditions and compared to the generalized Hoek-Brown criterion. A calculation sheet that implements the nonlinear methodology is presented and shared for digital download.

Keywords: Rock Mass Strength · Nonlinear Shear Strength · Rock Mechanics

1 Introduction

Rock mass strength is a required input parameter for many types of geotechnical analysis in the civil and mining industries. It is often impractical to measure rock mass strength directly, and therefore empirical failure criteria must be used in lieu of direct measurement. The CNI method is an empirical rock mass strength criterion based primarily on quantifiable input parameters. The premise of the method is that the rock mass strength can never be greater than the intact rock strength or less than the fracture shear strength, and therefore always lies in between the two. Strength testing has shown that interlocked materials such as rock masses often exhibit a nonlinear relationship between confining stress and strength, in particular at low normal stresses. This paper introduces a nonlinear formulation of the CNI method, building upon the linear formulation as described in Cylwik et al. 2022 [1]. The nonlinear criterion is formulated in terms of compressive strength, friction angle, and a curvature coefficient.

1.1 Review of CNI Method Linear Formulation

The equations to estimate the Mohr-Coulomb linear rock mass cohesion (coh_m), friction angle (ϕ_m), and rock mass compressive strength (σ_{cm}) are first reviewed since these parameters are used as direct inputs to the nonlinear formulation. The linear rock mass strength is estimated by combining the intact rock cohesion (coh_i) and friction angle (ϕ_i), and the fracture cohesion (coh_f) and friction angle (ϕ_f), with a weighting factor, r , that is based on the degree of fracturing within the rock mass as measured by either rock quality designation (RQD) or fracture frequency (λ). Equations 1 or 2 may be used to estimate r . The Mohr-Coulomb linear isotropic strength is estimated with Eqs. 3 to 5. The C_{rf} is an empirical cohesion adjustment parameter that typically varies from 0.25 to 0.5 for slope analysis and from 0.35 to 0.7 for underground analysis; it adjusts for scale effects and other factors that affect rock mass strength that are not accounted for by the primary quantifiable input parameters. A full review of the linear formulation is presented in [1], including selection of input parameters and limitations.

$$r = 0.05e^{0.026 \cdot RQD} \tag{1}$$

$$r = 0.05e^{(3 - 0.15 \cdot \lambda^{0.85})} \tag{2}$$

$$coh_m = C_{rf} [rcoh_i + (1 - r)coh_f] \tag{3}$$

$$\phi_m = \tan^{-1} \left[r^{2/3} \tan\phi_i + \left(1 - r^{2/3} \right) \tan\phi_f \right] \tag{4}$$

$$\sigma_{cm} = 2 \cdot coh_m \cdot \tan \left(45^\circ + \frac{\phi_m}{2} \right) \tag{5}$$

1.2 Discussion of Nonlinearity, Interlock, and Dilation

Interlocked materials tend to dilate significantly at low confinement, resulting in high apparent friction angles [2, 3]. As confinement increases, dilation is gradually suppressed, and instead intact strength is mobilized due to shearing through asperities and material crushing [4]. At very high confinements ($\sigma_3 > \sigma_{ci}$), the failure mode transitions to be dominated by plastic flow, resulting in low instantaneous friction angles. The nonlinear failure envelope of an interlocked material represents the overlapping transitions between different levels of dilation and different modes of shear failure.

A massive and undisturbed rock mass is highly interlocked, and therefore nonlinear strength behavior is expected. However, it has been demonstrated that the nonlinearity of a rock mass failure envelope can change if discontinuities (e.g., joints) are introduced parallel to the primary direction of shear stress [5]; the failure envelope becomes less curved and takes a hybrid shape between the intact and fracture envelopes (Fig. 1a). Modeling has shown that if smooth non-dilatant joints are added to a rock mass, the failure envelope tends to a more linear shape [3]. It has also been demonstrated that an increase in disturbance of a rock mass (i.e., less potential for dilation with shear)

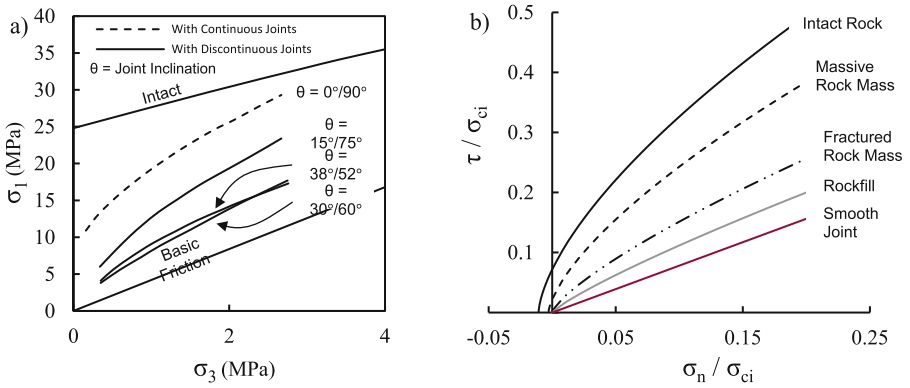


Fig. 1. a) Measured strength envelopes from biaxial tests of rock mass models with joints by [5], and b) Example normalized strength envelopes of materials with differing degrees of interlock

results in a less curved failure envelope [6]. A key feature of the CNI nonlinear method is that the degree of curvature of the failure envelope is transitional – it takes a form similar to intact rock for massive rock mass, and gradually transitions to a less curved failure envelope for highly fractured rock mass where shearing is expected primarily on joints rather than through solid material. An example of transitional envelope curvature is demonstrated for materials with varying degrees of interlock in Fig. 1b.

2 Generalized Nonlinear Criterion

The nonlinear formulation of the CNI method implements the generalized strength criterion shown in Eq. 6. The criterion was described in detail by Yu et al. [7] and originally proposed by Hoek and Brown [8]. The criterion is defined in terms of shear stress (τ) and normal stress (σ_n) and therefore can be readily implemented in slope stability analysis. The criterion contains two parameters with direct physical meaning defined as the uniaxial compressive strength (σ_c) and the direct tensile strength (T_o), and two dimensionless parameters defined as the strength magnitude coefficient (a) and the curvature coefficient (n). The parameter n is restricted to $0.5 < n < 1.0$ and defines the degree of curvature of the nonlinear envelope. When $n = 0.5$, the failure envelope has the maximum degree of curvature possible (an envelope with more curvature would violate Mohr failure laws [7]). For the case of $n = 1$, the criterion reduces to a linear Mohr-Coulomb relation.

$$\tau = \sigma_c \cdot a \left(\frac{\sigma_n}{\sigma_c} - \frac{T_o}{\sigma_c} \right)^n \tag{6}$$

A beneficial feature of this formulation is that all parameters in Eq. 6 can be defined in terms of compressive strength (σ_c), a characteristic friction angle (\emptyset), and n . The σ_c and friction angle of a rock mass are estimated with Eqs. 4 and 5. The parameter n is estimated empirically for the CNI method as described in the following chapter, where typical values of n are evaluated for many geological materials and used as the basis to estimate n for rock mass. Equations 7, 8, and 9 are derived directly from Mohr

failure theory as detailed in [7]. The equation derived by [7] to calculate n has been rearranged to solve for T_o in terms of σ_c , φ_c , and n (Eq. 7). The parameter φ_c is the instantaneous friction angle under a condition of uniaxial compression. The strength magnitude coefficient is calculated with Eqs. 8 and 9 and follows the derivations by [7].

$$T_o = \frac{\sigma_c}{2} \left(1 - \frac{n \cos \varphi_c}{\tan \varphi_c} - \sin \varphi_c \right) \tag{7}$$

$$a = \frac{\sqrt{(-A + 2n - 2\frac{T_o}{\sigma_c} - 1)(A + 2n + 2\frac{T_o}{\sigma_c} - 3)}}{4(1-n) \left(\frac{1}{2} - \frac{1 - 2\frac{T_o}{\sigma_c} - A}{4(1-n)} - \frac{T_o}{\sigma_c} \right)^n} \tag{8}$$

$$A = \sqrt{\left(1 - 2\frac{T_o}{\sigma_c} \right)^2 + 4n(n-1)} \tag{9}$$

The tangent point of the characteristic friction angle (\emptyset) is variable (unlike φ_c that has a fixed tangent point at the condition of uniaxial compression). Equation 10 serves to empirically shift the tangent point of \emptyset to higher normal stress ranges typically encountered in engineering analyses, where ρ_{atm} is defined as the atmospheric pressure. The tangent point of \emptyset is at lower stresses for weak materials and higher stresses for strong materials. Example strength envelopes showing different σ_c , \emptyset , and n values are presented in Fig. 2 and demonstrate the influence of the three input parameters.

$$\tan \varphi_c = \tan \emptyset \cdot \left(\frac{10 \cdot \rho_{atm}}{\sigma_c} \cdot \tan^{4-3n} \emptyset + \tan \emptyset - \sin \emptyset + 1 \right)^{\frac{1-n}{2n-1}} \tag{10}$$

The instantaneous major and minor principal stresses for a given τ - σ_n stress pair can be calculated with the solutions proposed by Balmer [9], as shown in Eqs. 11 to 13.

$$\sigma_1 = \sigma_n + \tau \cdot \tan \beta \tag{11}$$

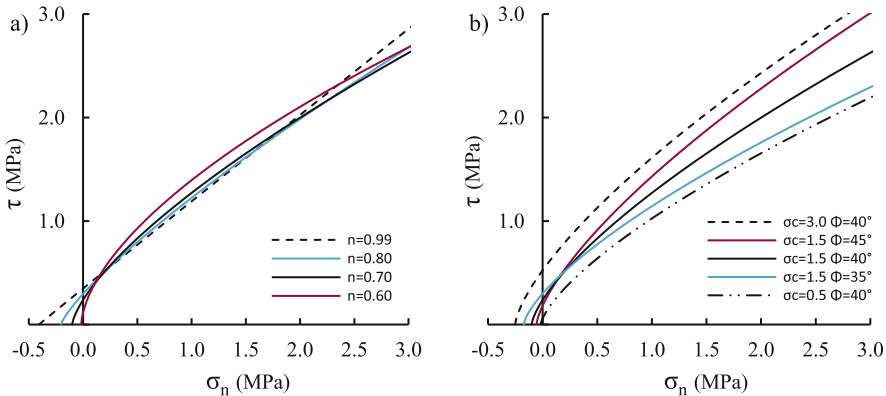


Fig. 2. Calculated strength envelope for $\sigma_c = 1.5$ MPa, $\emptyset = 40^\circ$, and $n = 0.70$ showing a) Sensitivity to n parameter, and b) Sensitivity to σ_c and \emptyset parameters

$$\sigma_3 = \sigma_n - \tau \cdot \frac{1}{\tan\beta} \quad (12)$$

$$\beta = \frac{1}{2} \tan^{-1} \left(\frac{d\tau}{d\sigma_n} \right) + \frac{\pi}{4} = \frac{1}{2} \tan^{-1} \left(n \cdot a \left(\frac{\sigma_n}{\sigma_c} - \frac{T_o}{\sigma_c} \right)^{n-1} \right) + \frac{\pi}{4} \quad (13)$$

3 Curvature Coefficient of Geological Materials and Rock Mass

In this chapter the parameter n is evaluated for geological materials that can be tested in the laboratory, since the value of n for a rock mass cannot be directly measured.

3.1 Intact Rock

To determine typical values of n for intact rock, the generalized nonlinear failure criterion was fit to 18 published sets of compression testing data. A full suite of triaxial testing data at various confinements was evaluated for each rock type with the input parameters σ_{ci} (intact compressive strength), \emptyset , and n considered variables for the regressions. A summary of the testing data is presented in Table 1. Example nonlinear models for six of the rock types are shown in Fig. 3a; similar quality fits were obtained for all rock types studied. Examination of the resulting σ_{ci} and n values shows no correlation (Fig. 4a). However, a strong positive correlation between \emptyset and n is observed as shown in Fig. 4b. It is hypothesized that dilation is suppressed more easily by confining stress for rocks with low \emptyset , resulting in a more curved failure envelope and therefore a lower n . An empirical model to estimate n for intact hard rock is shown as Eq. 14 and in Fig. 4b. Post-peak triaxial testing on intact rock was also examined as shown in Figs. 3b and 4b. Each data point on Fig. 4b represents a suite of residual triaxial tests on one rock type, with multiple post-peak confinements tested for each sample.

$$n_{\text{intact-hardrock}} \approx \frac{1}{2} \left[1 + \sin^2 \emptyset \right] \quad (14)$$

3.2 Weak Rock

Most rock classification systems define the transition between hard rock and weak rock to be between a σ_{ci} of 15 to 25 MPa, and the boundary between soil and soft rock to be between 0.5 and 2 MPa [35]. Many authors have noted that strength criteria designed for hard rock may not perform satisfactorily for weak rock, as weak rocks often exhibit failure envelopes that are less curved [24]. However, existing data supports the idea that there is a smooth transition between the drained strength behavior of hard rock, soft rock, and dense soil [35]. Twenty suites of triaxial testing were examined for weak rocks as summarized in Table 1. The $\tan\emptyset$ and n values obtained from regressions of the test results are shown in Fig. 5 and are compared to the data from hard rocks. In general, rocks with lower σ_{ci} result in strength envelopes with higher n values (i.e., closer to linear). The empirical model to estimate n can be improved by incorporating σ_{ci} as

Table 1. Summary of laboratory testing data modeled with the generalized nonlinear criterion

Material Type	Test Type	No. of Data Sets	Typical \emptyset	Typical n	Data Source
Intact Rock	Peak Triaxial	18	33° - 54°	0.56 - 0.72	Granite [8, 10, 11, 12, 13], Limestone [10, 11, 14], Marble [11, 15, 16], Sandstone [8, 17], Salt [18, 19], Dolerite [11], Potash [10], Dolomite [14]
Intact Rock (Weak Rock)	Peak Triaxial	20	33° - 50°	0.67 - 0.82	Mudstone [20, 21], Mudrock [22], Quartzitic Sandstone [23], Marlstone [24]
Intact Rock	Post-Peak Triaxial	13	28° - 53°	0.64 - 0.83	Internal CNI Laboratory Testing
Saprolite / Residual Soil-Rock	CD-Triaxial, Ring Shear	10	9° - 30°	0.82 - 0.95	Granitic residual soil [25], Residual soils of basalt and dacite [26], Ash [27]
Rockfill	Triaxial	11	36° - 44°	0.85 - 0.90	[28–30]
Sand	Triaxial	10	36° - 42°	0.88 - 0.95	[31–33]
Rock Joints	Barton Model	13	33° - 48°	0.84 - 0.95	[34]

shown in Eqs. 15 and 16 and in Fig. 5. The observed increase in n due to a reduction in σ_{ci} is captured, and the trend of increased n for higher $\tan\emptyset$ is also honored. Example failure envelopes showing the decrease in curvature with σ_{ci} are presented in Fig. 6a, and example implementation of the model for some of the published weak rock triaxial testing is shown in Fig. 6b.

$$n_{intactrock} \approx \frac{1}{2} [1 + \sin^{\chi} \emptyset] \tag{15}$$

$$\chi \approx \frac{7}{2} \left[1 - 0.5^{50 \frac{\sigma_{ci}}{\rho_{atm}}} \right] \tag{16}$$

Figure 6a Calculated strengths for $\emptyset = 35^\circ$ showing failure envelope curvature sensitivity to σ_{ci} , and b) Example generalized nonlinear criterion models compared to testing data for weak rocks

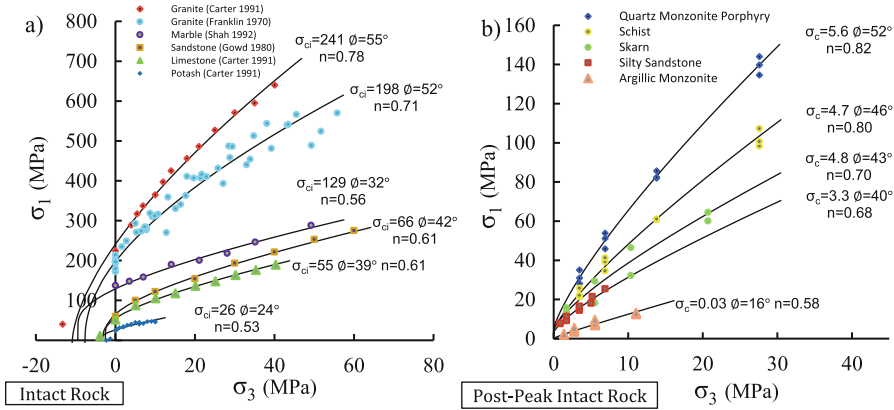


Fig. 3. Example generalized nonlinear criterion models compared to testing data for a) Peak triaxial strength of intact rock, and b) Post-peak triaxial strength of intact rock

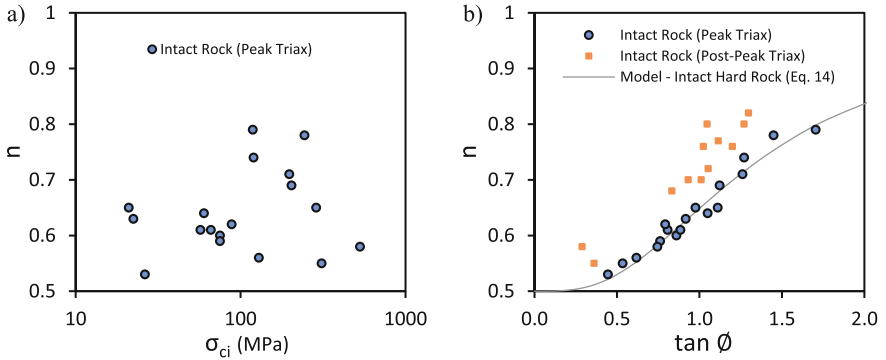


Fig. 4. Curvature coefficient (n) for intact rock compared to a) σ_{ci} , and b) $\tan \phi$

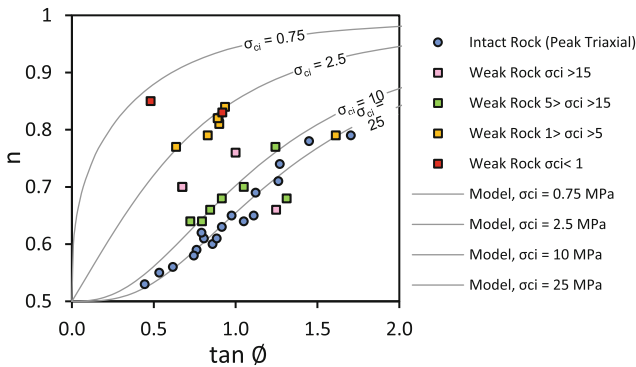


Fig. 5. Curvature coefficient (n) for weak rocks versus $\tan \phi$ with proposed model (Eq. 15)

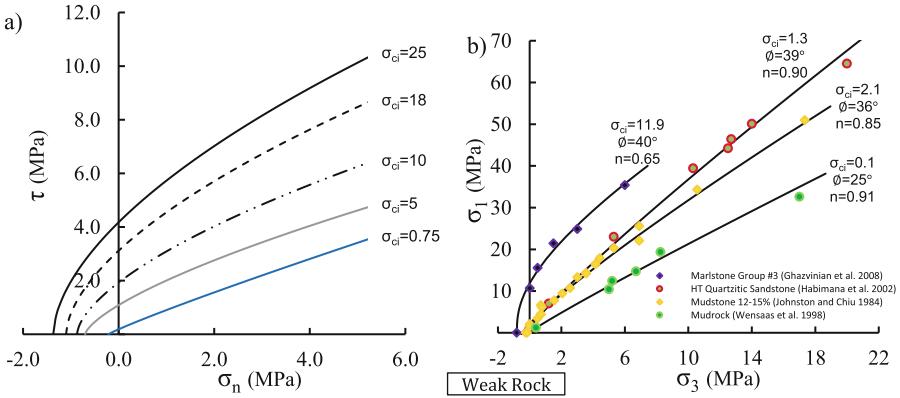


Fig. 6. a) Calculated strengths for $\phi = 35^\circ$ showing failure envelope curvature sensitivity to σ_{ci} , and b) Example generalized nonlinear criterion models compared to testing data for weak rocks

3.3 Saprolite, Sand, Rockfill, and Rock Joints

Other geological materials that have extensive published testing databases were examined to determine typical nonlinear parameters, including saprolite, sand, rockfill, and rock joints (Table 1). Examples of the criterion compared to testing data are shown in Fig. 7. The nonlinear criterion is able to model all material types examined. Measured n values were significantly higher for these materials compared to intact rock. It can be seen that n increases with decreasing particle size (e.g., rockfill to sand), and decreases with increased compaction and interlock. Saprolite (residual rock/soil) was examined with ten suites of triaxial or ring shear testing and resulted in lower ϕ values than other materials and failure envelopes that ranged from linear to slightly curved ($n > 0.8$). For sand, higher relative densities resulted in more curved envelopes, with ϕ values ranging from 33 to 44 degrees. Eleven rockfill shear strength models were fit with the nonlinear criterion and resulted in slightly higher ϕ values and lower n values than sand. The Leps [28] rockfill strength curves can be effectively modeled with the criterion as shown in Fig. 7c. Rock joints were examined by considering the Barton and Choubey joint strength model [34] with joint roughness coefficient (JRC) values varied from 1 to 15. Example joint shear strength curves are fitted in Fig. 7d, with higher JRC values resulting in lower n values and higher ϕ values. The envelope curvature and friction angle for rock joints is seen to have a wide potential range of values. It is possible for rock joints to be weak/smooth/low dilation (low ϕ and high n) at one end of the spectrum, or strong/rough/high dilation (high ϕ and low n) at the other.

3.4 Estimation of the Curvature Coefficient for Rock Mass

All data analyzed for this study are plotted in Fig. 8, highlighting the relationships between dilation/interlock, frictional strength, and failure envelope curvature for different geological materials. The measured values of n for different material types may be used to bracket the likely range of n for rock mass. The intact rock weighting factor (r) used in the CNI method is a measure of the level of jointing or blockiness of a rock mass

and can therefore be used to predict the degree of failure on pre-existing joint planes during shear of a rock mass. The proposed empirical model for n for use in rock mass strength estimation is shown in Eq. 17 and transitions smoothly from intact rock ($r = 1$) to the soil-rock transition zone ($r = 0.01$) as a rock mass becomes more jointed. The model accounts for the decrease in curvature of the failure envelope with increasing \emptyset , the decrease in curvature for weaker rocks, and the anticipated decrease in curvature as more sliding takes place on pre-existing joint planes. Based on all the test data analyzed for this study, typical regions for different material types are shown on a $\tan\emptyset$ versus n chart in Fig. 9.

$$n_{rockmass} \approx \frac{1}{2} \left[1 + \sin^X \emptyset + (1 - \sin^X \emptyset) (1 - r^{0.15})^{\cos \emptyset} \right] \tag{17}$$

Figure 8 Curvature coefficient (n) versus $\tan\emptyset$ for all material types evaluated

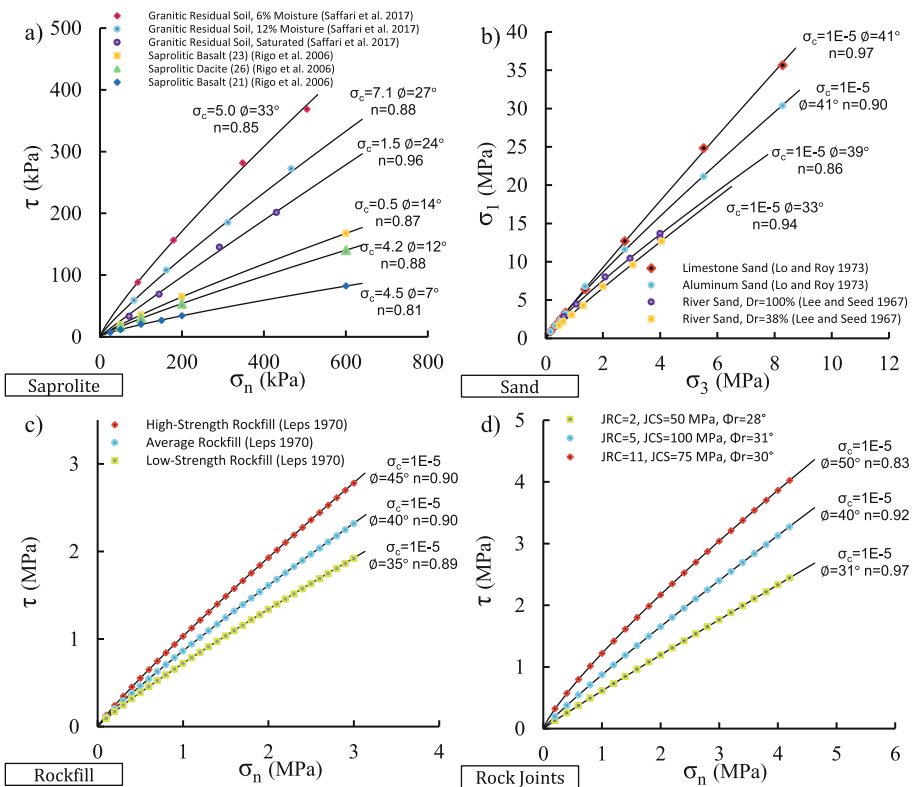


Fig. 7. Example generalized nonlinear criterion models compared to testing data and models for a) Sapolite, b) Sand, c) Rockfill, and d) Rock Joints

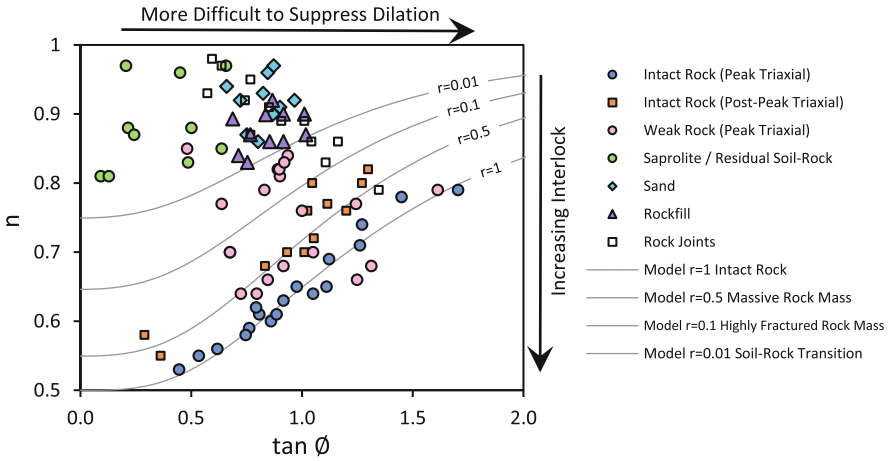


Fig. 8. Curvature coefficient (n) versus $\tan\phi$ for all material types evaluated

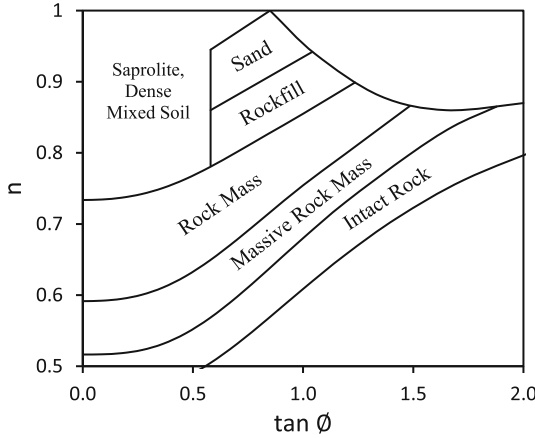


Fig. 9. Predicted regions of curvature coefficient (n) and $\tan\phi$ for different geological material types

4 Example Rock Mass Strength Estimation

The strength of an example sandstone rock mass (Table 2) is estimated using the nonlinear CNI method. Figure 10 shows the estimated strength of the rock mass in addition to families of curves demonstrating sensitivities to the input parameters (note the plots are in shear-normal stress space since this is the native form of the strength criterion). Raising or lowering σ_{ci} of the intact rock does not alter the shape or inclination of the failure surface and only affects the estimated cohesion of the rock mass (Fig. 10a). As ϕ_i or ϕ_f change, the inclination of the failure envelope is modified with a common tangent point near the rock mass cohesion (Fig. 10b). Because the n value is a function of the friction angle, the estimated tensile strength does not change significantly with variations

Table 2. Properties of the example rock masses

Rock Type	Σc_i (MPa)	θ_I (deg.)	coh_i (MPa)	θ_f (deg.)	RQD (%)	Λ (frac/m)	Cr _f	m_i	GSI
Limestone	94	41	21.4	30	90	5.7	0.5	8.9	69
Sandstone	66	42	14.7	32	60	14.3	0.5	11	58
Granite	198	51	35.1	29	35	22.2	0.5	21	41
Marble	75	37	18.7	28	10	30.5	0.5	5.4	30

in either input friction angle. Changing the input RQD or fracture frequency affects the rock mass cohesion, envelope inclination, and shape of the failure envelope (Fig. 10c). The failure envelope is less curved for highly fractured rock mass and more curved for massive rock mass. The Cr_f acts as a simple multiplier of the cohesion of the rock mass (Fig. 10d) and does not alter the shape or inclination of the failure surface. A discussion regarding the selection of Cr_f can be found in [1].

5 Comparison to Hoek-Brown Criterion

The Hoek-Brown empirical rock mass strength criterion was first introduced in 1980 [8] and has been modified and updated many times since then, with the most recent publication in 2019 [36]. A historical review of the Hoek-Brown criterion development was presented in [37]. A primary comparison between the linear CNI method and the generalized Hoek-Brown criterion was presented in 2022 [1], and those findings are not repeated in this publication. Additional comparisons and conclusions are presented herein, especially those pertaining to the nonlinearity of the two criteria.

5.1 Direct Estimation Comparisons

Estimated rock mass strength envelopes for the four rock masses listed in Table 2 are shown in Fig. 11 for the 1) CNI method with $Cr_f = 0.5$, and 2) generalized Hoek-Brown criterion with D ranging from 0 to 1. The CNI method strengths generally plot in between the $D = 0$ and $D = 1$ Hoek-Brown envelopes, except at very low confining stresses where the CNI method predicts higher shear strengths. The only exception to this is for the massive limestone (Fig. 11a), where the CNI method strength envelope plots above the Hoek-Brown curves for normal stresses less than 8 MPa. The higher estimated strength may be desirable, as recent studies have demonstrated that the strength of non-persistently jointed rock masses ($GSI > 65$) may be underpredicted by the Hoek-Brown criterion [3]. For weaker rock masses, CNI method strengths typically increase relative to Hoek-Brown strengths. This is the case for the marble ($GSI = 30$), where the CNI method is closer to the Hoek-Brown $D = 0$ undisturbed curve. For a rock mass with a low GSI rating, high D values can result in very low strength estimates [1, 6]. The CNI method plots just above the $D = 1$ curve for the granite. This occurs because the CNI method weights the fracture strength more heavily for highly fractured rock masses, and

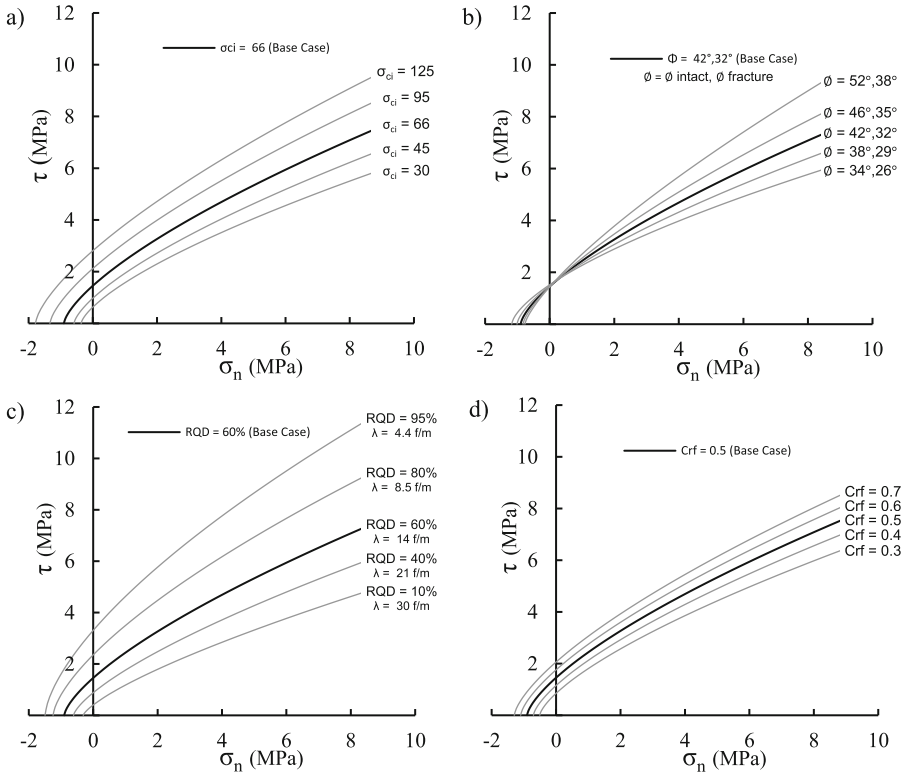


Fig. 10. Calculated strength envelopes with the nonlinear CNI method for the example sandstone rock mass showing sensitivity to the input parameters of a) Intact rock compressive strength, b) Intact and fracture friction angles, c) RQD or fracture frequency, and d) Crf

the generalized Hoek–Brown criterion uses m_i to determine the inclination of the failure envelope regardless of the GSI value.

5.2 Comparison of Nonlinearity

The nonlinear criterion is also able to emulate the generalized Hoek-Brown criterion in the compressive stress range as shown for three example rock masses in Fig. 12, where σ_{cm} is the rock mass compressive strength. Strength envelopes for rocks with σ_{ci} ranging from 25 to 200 MPa and m_i from 5 to 35 were generated with the Hoek-Brown criterion for intact rock and fit using the generalized nonlinear criterion; the resulting $\tan\theta$ and n values to model the Hoek-Brown intact curves are shown in Fig. 13a. The Hoek-Brown intact criterion follows a similar trend to Eq. 14 of positive correlation between n and $\tan\theta$, but with a different slope and shape than observed from the testing data analyzed for this study. Inspection of Fig. 13a reveals that the CNI method predicts failure envelopes with more curvature (i.e., less tensile strength) when the m_i value is less than 10. Note that a tension cut-off was not required to model any of the compression testing data with the generalized nonlinear criterion.

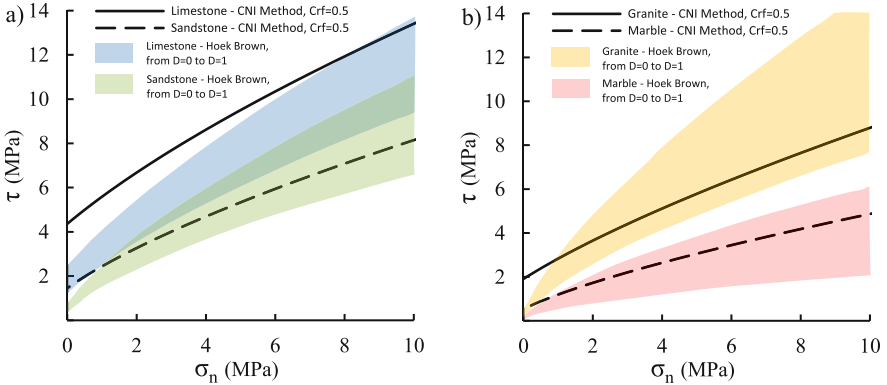


Fig. 11. Comparison of CNI method to generalized Hoek-Brown criterion for example rock masses a) Limestone and sandstone, and b) Granite and marble

The nonlinear criterion was also fit to a suite of generalized Hoek-Brown curves for rock masses with GSI ranging from 25 to 85 and with a D of either 0 or 1. It can be seen in Fig. 13b that the generalized Hoek-Brown criterion for rock masses produces strength envelopes with the same degree of nonlinearity (curvature) as the intact Hoek-Brown criterion, with n values restricted to a range of 0.6 to 0.7 for all reasonable combinations of rock mass input parameters. Consequently, there is no combination of generalized Hoek-Brown input parameters that will produce a failure envelope to model a material with a higher n value, such as compacted rockfill. Alternatively, strength envelopes from the CNI method become less curved and more similar to a linear envelope as more fracturing is modeled within a rock mass.

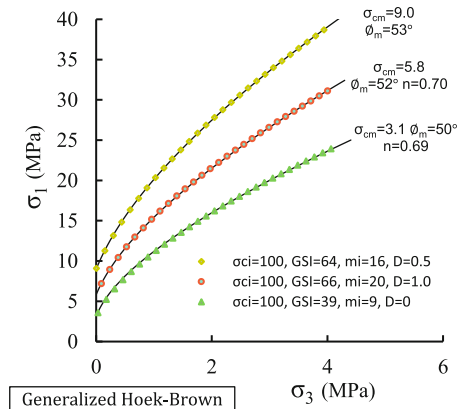


Fig. 12. Example nonlinear criterion models fit to three different generalized Hoek-Brown criterion strength envelopes

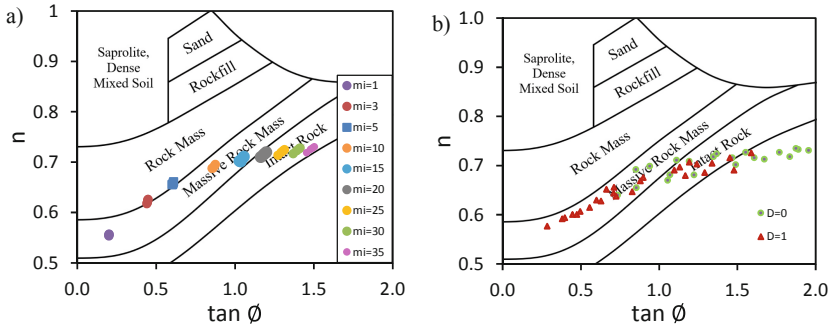


Fig. 13. Curvature coefficient (n) versus $\tan\phi$ for a) Intact Hoek-Brown criterion with various m_i and σ_{ci} values, and b) Generalized Hoek-Brown criterion with $D = 0$ and $D = 1$ for various rock mass properties

5.3 Comparison of Input Parameters

Cross-correlation coefficients between the input and output parameters were calculated for a set of rock masses with either 60% or 10% RQD using the CNI method, as shown in Table 3. Examination of the cross-correlation coefficients can reveal the influence that each input parameter exerts on the results. The generalized nonlinear criterion was also fit to a series of generalized Hoek-Brown curves with a GSI of either 50 or 25, and the cross-correlation coefficients between the input and output parameters are shown in Table 4. Key observations and comparisons are summarized below.

- For the CNI method, coh_i affects σ_{cm} , ϕ_i and ϕ_f affect $\tan\phi_m$ and n , and RQD or λ affects all three output parameters.
- Within the CNI method, ϕ_i is the primary control on $\tan\phi_m$ for massive rock masses, and a transition is made for ϕ_f to control $\tan\phi_m$ for highly fractured rock masses where shear will primarily take place along pre-existing joints. Within the generalized Hoek-Brown criterion, the parameter m_i is shown to be the primary control on $\tan\phi_m$ regardless of the rock mass quality. The fracture condition cannot be treated as an independent parameter within the Hoek-Brown system since it is incorporated as a component of the GSI rating system.
- It is seen that GSI has the most significant influence on σ_{cm} and that m_i has the most control over $\tan\phi_m$.
- An unexpected result is the negative correlation between n and D (the Hoek-Brown disturbance parameter). As a rock mass becomes more disturbed/damaged, less interlocking and less dilation would be anticipated and therefore a less curved failure envelope (i.e., higher n). This correlation is also shown graphically in Fig. 13b.
- The Hoek-Brown D parameter has significantly more influence over the output parameters at lower GSI values. This has also been demonstrated by [1, 6], and [38].

5.4 Peak Strength Versus Post-Peak Strength

The CNI method was originally developed through calibration to open pit slope failure and underground pillar failure case histories (an example case history was presented by

Table 3. Cross-correlation coefficients between input and output parameters with the CNI method

Outputs	For RQD = 60%, $\lambda = 14$ frac/m			For RQD = 10%, $\lambda = 31$ frac/m		
	σ_{cm}	$\tan\theta_m$	n	σ_{cm}	$\tan\theta_m$	n
coh_i	0.7	0	0	0.7	0	0
θ_i	0.2	0.8	0.8	0.1	0.5	0.4
θ_f	0.1	0.4	0.5	0.2	0.9	0.8
RQD, λ^{-1}	0.5	0.3	-0.4	0.3	0.1	-0.4
Crf	0.4	0	0	0.5	0	0

Table 4. Cross-correlation coefficients between input and output parameters with the generalized Hoek-Brown criterion

Outputs	For GSI = 50			For GSI = 25		
	σ_{cm}	$\tan\theta_m$	n	σ_{cm}	$\tan\theta_m$	n
σ_{ci}	0.2	0.3	0.5	0.5	0.4	0.4
GSI	0.8	0.2	0.3	0.6	0.3	0
m_i	0	0.8	0.6	0	0.5	0.5
D	-0.2	-0.4	-0.5	-0.6	-0.6	-0.7

Nutakor et al. [39]). Most large rock slope failures experience significant displacement before ultimate collapse occurs [40], meaning that ultimate failure occurs after peak strengths have been mobilized. The CNI method is therefore neither an estimate of the peak or residual strength, but is considered a post-peak strength that lies somewhere in between the two extremes. The CNI method predicts the shear strength that will be realized on the critical shear plane at the time of collapse (if a failure is to occur). This contrasts with the generalized Hoek-Brown criterion, which is explicitly defined as a peak strength envelope [8]. For rock masses that will not be mobilized to failure, the CNI method will provide a conservative estimate of strength, especially far away from the excavation where plastic strains will be minimal. For models that employ only a single strength value (i.e., no strain-softening), it may be considered unsafe to design on peak strengths alone unless a high factor of safety value is required [41].

6 Conclusions

Rock mass strength is a required input parameter for many analyses in hard rock geotechnics. The strength criterion described by Yu et al. [7] is used as the basis to define the CNI method of rock mass strength estimation in nonlinear form. The utility of the criterion lies in the simplicity and familiarity of its input parameters. It provides a framework to describe the nonlinear strength of rock masses and many other geological materials with three easy to understand parameters. The first two parameters are those most familiar to

the rock mechanic and engineering geologist – compressive strength and friction angle. A third parameter, n , describes the degree of nonlinearity of the failure envelope, and ranges from 0.5 (maximum curvature) to 1.0 (linear). The generalized strength criterion has been fit to over 80 suites of published testing data and shown to effectively model many material types, including intact hard rock, weak rock, saprolite, sand, rockfill, and rock joints. The results show that the nonlinearity of the failure envelope is directly related to the degree of interlock and friction angle of the material. The simplicity of the system empowers the practitioner to exercise engineering judgement, since the curvature parameter can be reasonably selected for rock mass or any other geological material based on anticipated interlock and potential for dilation.

A key characteristic of the CNI nonlinear method is that the degree of curvature of the failure envelope is transitional. It takes a form similar to intact rock for massive rock mass, and gradually transitions to a less curved failure envelope for highly fractured rock mass where shearing is expected primarily on joints rather than through intact rock. When all examined material types are plotted on a chart of friction angle versus curvature of the failure envelope, it is seen that there is a smooth transitional relationship between intact rock, soft rock, and dense soil. These transitions are inherent to the nonlinear formulation of the CNI method. The procedure for estimation of strength is flexible; any of the equations for compressive strength, friction angle, or curvature coefficient may be updated independently as new information becomes available in the future.

6.1 Calculation Worksheet

A worksheet has been created that performs the nonlinear CNI method rock mass calculations presented herein. The worksheet is available for public download at the website “<https://www.cnitucson.com/publications.html>” [42].

Acknowledgements. The authors thank every researcher who published laboratory testing data that was referenced within this article. Without their contributions this paper would not have been possible. The authors also acknowledge the anonymous reviewers, Dr. Hossein Rafiei Renani, Dr. Loren Lorig, and Dr. Derek Martin who helped improve the quality of this manuscript.

References

1. Cylwik, S.D., Killian, J.R., Cicchini, P.F.: A practical strength criterion for rock masses based on quantitative input parameters. In: Slope Stability 2022, October 17–21, 2022, Tucson, AZ, USA (2022).
2. Ladanyi, B., Archambault, G.: Simulation of shear behavior of a jointed rock mass. In: The 11th US Symposium on Rock Mechanics (USRMS), OnePetro (1969).
3. Bahrani, N., Kaiser, P.K.: Influence of degree of interlock on confined strength of jointed hard rock masses. *Journal of Rock Mechanics and Geotechnical Engineering*, 12(6), pp. 1152-1170 (2020).
4. Barton, N.: Nonlinear shear strength for rock, rock joints, rockfill and interfaces. *Innovative Infrastructure Solutions*, 1, 1-19 (2016).

5. Ladanyi, B. Archambault, G.: Direct and indirect determination of shear strength of rock mass. In: AIME Annual Meeting, Las Vegas, Nevada, Feb 24–28, 1980, Preprint, (80–25), pp. 24–28 (1980).
6. Lorig, L., Potyondy, D., Varun.: Quantifying excavation-induced rock mass damage in large open pits. In: P.M. Dight (ed.), *Slope Stability 2020: Proceedings of the 2020 International Symposium on Slope Stability in Open Pit Mining and Civil Engineering*, Australian Centre for Geomechanics, Perth, pp. 969–982 (2020).
7. Yu, H., Ng, K., Grana, D., Alvarado, V., Kaszuba, J., Campbell, E.: A generalized power-law criterion for rocks based on Mohr failure theory. *International Journal of Rock Mechanics and Mining Sciences*, 128, 104274 (2020).
8. Hoek, E., Brown, E.T.: Empirical strength criterion for rock masses. *J Geotech Engineering, ASCE*, 106(GT9), 1013– 1035 (1980).
9. Balmer, G.: A General Analytical Solution for Mohr’s Envelope. *Proceedings of American Society of Test Materials*, Vol. 52, 1260-1271 (1952).
10. Carter, B.J., Scott Duncan, E.J., Lajtai, E.Z.: Fitting strength criteria to intact rock. *Geotech Geol Eng* 9, 73–81 (1991).
11. Franklin, J.A., Hoek, E.: Developments in triaxial testing technique. *Rock Mechanics*, 2(4), pp.223-228 (1970).
12. Walton, G., Diederichs, M., Punkkinen, A., Whitmore, J.: Back analysis of a pillar monitoring experiment at 2.4 km depth in the Sudbury Basin, Canada. *International Journal of Rock Mechanics and Mining Sciences*, 85, 33–51 (2016).
13. Alejano L.R., Arzúa J., Bozorgzadeh, N., Harrison J.P.: Triaxial strength and deformability of intact and increasingly jointed granite samples. *Int. J. Rock. Mech. & Min. Sci.* 95, 87–103 (2017).
14. Handin, J., Heard, H.C., Magouirk, J.N.: Effects of the intermediate principal stress on the failure of limestone, dolomite, and glass at different temperatures and strain rates. *Journal of Geophysical Research*, 72(2), 611– 640 (1967).
15. Fredrich, J.T., Evans, B., and Wong, T.F.: Micromechanics of the brittle to plastic transition in Carrara marble, *J. Geophys. Res.*, 94(B4), 4129– 4145 (1989).
16. Shah, S., Hoek, E.: Simplex reflection analysis of laboratory strength data. *Canadian Geotechnical Journal*, 29(2), pp.278-287 (1992).
17. Gowd T.N., Rummel, F.: Effect of confining pressure on the fracture behaviour of a porous rock. *Int J Rock Mech Min Sci Geomech Abstr* 17, 225–229 (1980).
18. Liu, X.Y., Ma, L.J., Ma, S.N., Zhang, X.W., Gao, L.: Comparative study of four failure criteria for intact bedded rock salt. *International Journal of Rock Mechanics and Mining Sciences*, 48(2), pp.341-346 (2011).
19. Sriapai, T., Walsri, C., Fuenkajorn, K.: True-triaxial compressive strength of Maha Sarakham salt. *Int. J. Rock Mech. Min.* 61, 256–265 (2013).
20. Johnston, I.W., Chiu, H.K.: Strength of Weathered Melbourne Mudstone. *Journal of Geotechnical Engineering*, 110, 875-898 (1984).
21. Chen, P. Y., Lee, D. H., Wu, J. H., Chen, J. J.: Investigating the mechanical behavior of mudstone subjected to cyclical loading. 356 – 365 (2010).
22. Wensaas, L., Aagaard, P., Berre, T., Roaldset, E.: Mechanical properties of North Sea Tertiary mudrocks: investigations by triaxial testing of side-wall cores. *Clay Minerals*, 33, 171 – 183 (1998).
23. Habimana, J., Labiouse, V., Descoedres, F.: Geomechanical characterisation of cataclastic rocks: experience from the Cleuson–Dixence project. *International Journal of Rock Mechanics and Mining Sciences*, 39, 677-693 (2002).
24. Ghazvinian, A., Fathi, A., Moradian, Z.: Failure behavior of marlstone under triaxial compression. *International Journal of Rock Mechanics and Mining Sciences*, 45, 807-814 (2008).

25. Saffari, P., Noor, M. J.M., Motamedi, S., Hashim, R., Ismail, Z., Hadi, B.A.: Experimental study on nonlinear shear strength behavior of a tropical granitic residual soil (Grade VI) at various initial moisture contents. *Jurnal Teknologi*, 79(2) (2017).
26. Rigo, M.L., Pinheiro, R.J.B., Bressani, L.A., Bica, A.V.D., Silveira, R.M.D.: The residual shear strength of tropical soils. *Canadian Geotechnical Journal*, 43(4), 431-447 (2006).
27. Gan, J.K., Fredlund, D.G.: Shear strength characteristics of two saprolitic soils. *Canadian Geotechnical Journal*, 33(4), 595-609 (1996).
28. Leps, T.M.: Review of shearing strength of rockfill. *J. Soil Mech. Found. Div. ASCE* 96, No. SM4, 1159–1170 (1970).
29. Indraratna, B., Wijewardena, L. S.S., Balasubramaniam, A.S.: Large-scale triaxial testing of grey wacke rockfill. *Geotechnique*, 43(1), 37-51 (1993).
30. Ovalle, C., Linero, S., Dano, C., Bard, E., Hicher, P.Y., Osses, R.: Data compilation from large drained compression triaxial tests on coarse crushable rockfill materials. *Journal of Geotechnical and Geoenvironmental Engineering*, 146(9), 06020013 (2020).
31. Lee, K.L., Seed, H.B.: Drained strength characteristics of sands. *Journal of the Soil Mechanics and Foundations Division*, 93(6), 117-141 (1967).
32. Lo, K.Y., Roy, M.: Response of particulate materials at high pressures. *Soils and Foundations*, 13(1), 61-76 (1973).
33. Desrosiers, R., Silva, A.J.: Strength behavior of marine sands at elevated confining stresses. *Marine Georesources and Geotechnology*, 20(1), 1-19 (2002).
34. Barton, N., Choubey, V.: The shear strength of rock joints in theory and practice. *Rock mechanics*, 10(1), 1-54 (1977).
35. Kanji, M. A.: Critical issues in soft rocks. *Journal of Rock Mechanics and Geotechnical Engineering*, 6(3), 186–195 (2014).
36. Hoek, E., Brown, E.T.: The Hoek–Brown failure criterion and GSI–2018 edition. *J Rock Mech Geotech Eng.* 11(3), 445- 463 (2019).
37. Rafiei Renani, H., Cai, M.: Forty-Year Review of the Hoek–Brown Failure Criterion for Jointed Rock Masses. *Rock Mechanics and Rock Engineering*, 1–23 (2022).
38. Li, A.J., Merifield, R.S., Lyamin, A.V.: Effect of rock mass disturbance on the stability of rock slopes using the Hoek–Brown failure criterion. *Computers and Geotechnics*, 38(4), 546-558 (2011).
39. Nutakor, D., Asbury, N., Zavodni, Z.: Back analysis of Rio Tinto Borates and Lithium Mine north wall failure. In: *Slope Stability 2022*, October 17–21, 2022, Tucson, AZ, USA (2022).
40. Sharon, R., Eberhardt, E. (eds.): *Guidelines for Slope Performance Monitoring*. CSIRO Publishing (2020).
41. Budhu, M.: *Soil mechanics and foundations* (No. Ed. 3). John Wiley & Sons (2010).
42. Call & Nicholas, Inc. Publications Page, <https://www.cnitucson.com/publications.html>, last accessed 2023/04/24.

Open Access This chapter is licensed under the terms of the Creative Commons Attribution-NonCommercial 4.0 International License (<http://creativecommons.org/licenses/by-nc/4.0/>), which permits any noncommercial use, sharing, adaptation, distribution and reproduction in any medium or format, as long as you give appropriate credit to the original author(s) and the source, provide a link to the Creative Commons license and indicate if changes were made.

The images or other third party material in this chapter are included in the chapter's Creative Commons license, unless indicated otherwise in a credit line to the material. If material is not included in the chapter's Creative Commons license and your intended use is not permitted by statutory regulation or exceeds the permitted use, you will need to obtain permission directly from the copyright holder.

